Desalination and Water Treatment
www.deswater.com
doi: 10.5004/dwt.2021.26984

220 (2021) 309–315
April

FeAlPO-34 molecular sieves with controllably high iron contents: ionothermal synthesis and catalytic performance in phenol hydroxylation

Liang Zhou[a], Hongjian Li[a], Jinqu Wang[a], Runlin Han[a,b,*]

[a]*School of Chemical Engineering, Dalian University of Technology, Dalian 116024, China, Tel. +86-13842712519; emails: hanrunlin@163.com (R. Han), zhouliang@dlut.edu.cn (L. Zhou), lihongjian420@163.com (H. Li), wangjq@dlut.edu.cn (J. Wang)*[b]*School of Chemistry and Chemical Engineering, Jinggangshan University, Ji'an 343009, China*

Received 21 July 2020; Accepted 21 December 2020

ABSTRACT

FeAlPO-34 molecular sieves with tunable iron contents were synthesized in a 1-butyl-3-methylimidazolium bromide [BMIm]Br ionic liquid. The added Fe^{3+} was successfully incorporated into the AlPO-34 framework, which mainly presents in tetrahedral and octahedral sites in the framework, with up to 10.28 wt.% of isolated iron contents. The iron contents directly influenced the crystal size and morphology, mesoporous properties. A sample with relatively high iron contents and a hierarchical structure shows excellent catalytic performances when utilized as the catalyst of phenol hydroxylation reaction. The sample with 6.09 wt.% Fe showed a 41.55% of phenol conversion with the selectivity of 92.72 to hydroquinone and catechol.

Keywords: FeAlPO-34; Ionothermal synthesis; Phenol hydroxylation; Ionic liquid

1. Introduction

Zeolites and zeotypes are widely used microporous materials with three-dimensional open frameworks. They have been broadly exploited as shape-selective catalysts, sorbents and ion exchangers due to their structural variability, high specific surface area, pore diameter, and ion exchange sites [1–3]. Among these materials, the aluminophosphates (AlPOs) are microporous inorganic materials constituted by alternated AlO_4^- and PO_4^- tetrahedral with a structural neutral charge. The uniform frameworks of AlPOs provide a relatively excellent chemical stability, hydrothermal stability and thermal stability. However, the neutral structure limits, to a great extend, their catalysis and ion-exchange functionality [4]. Fortunately, heteroatoms such as Si^{4+}, Fe^{3+}, Co^{3+}, Zn^{2+}, etc. can be incorporated into AlPOs' frameworks and serve as active sites in heterogeneous catalysts [5,6]. Increasing heteroatom content in frameworks is always a crucial topic in the preparation of metalloaluminophosphates (MeAPOs) catalyst since an increase of active sites enhances the catalytic activity. However, MeAPOs are commonly prepared via a hydrothermal approach in a sealed autoclave under a high autogenous pressure condition [7,8]. The very low solubility of the heteroatoms under highly basic conditions in hydrothermal synthesis makes the fabrication of high heteroatom content molecular sieves difficult [9]. Furthermore, the safety issues of hydrothermal synthesis cannot be ignored.

A novel zeolitic molecular sieves synthesis method, known as the ionothermal synthesis method, enables the fabrication of zeolites via atmospheric pressure synthesis, due to the negligible vapor pressure of the ionic liquid solvents [10,11]. During the ionothermal synthesis process, there is no additional water introduced thus reducing the hydrolysis of the heteroatom salt. Besides, in imidazolium bromide ionic liquids, heteroatom cations adequately dissolve by weak interactions with bromide anions [12]. Based on the above characteristics, a series of MeAPOs with high

* Corresponding author.

amounts of heteroatom has been successfully synthesized via ionothermal synthesis routes [13,14]. It is well established that iron-containing aluminophosphate molecular sieves (designated FeAlPOs) is one of the most attractive materials among the various MeAPOs. Fe^{3+} occurring in the synthesis gel incorporates into "AlO_4" tetrahedron according to SM Ic substitution modes [15]. FeAlPOs show considerably remarkable ability in many catalysis reactions [16].

Phenolic compounds are important raw materials in the preparation of pesticides, resins and antioxidants [17]. However, the highly toxic phenolic wastewater is difficult to treat with traditional biodegradation. Strong chemical treatment also has the problem of low efficiency and high cost [18]. The development of new materials with special structures and high performance in wastewater treatment attracts more and more attention [19]. For the reaction of phenol hydroxylation, the iron contents directly affect the conversion of the phenol and the selectivity of hydroquinone. FeAlPOs with a microporous structure and certain content of Fe ion will promote the reaction which is meaningful to the phenol wastewater treatment. However, there is no reference about phenol hydroxylation with FeAlPOs as far as we know.

In this work, diverse Fe/Al ratios in the initial compositions were utilized for varying the probability of Fe^{3+} replacing Al^{3+} in the "AlO_4" tetrahedron and successfully synthesized a series of FeAlPO-34 with various and relatively high contents as well as isolated iron contents via ionothermal approach. Catalytic performance of the FeAlPO molecular sieves in the phenol reaction was studied and the effect of Fe content was investigated in detail.

2. Experimental

2.1. Synthesis

The typical synthesis procedure of FeAlPO-34 can be described as follows: the synthesis solution was prepared by mixing 27.1 g (0.1 mol) of 1-butyl-3-methylimidazolium bromide ([BMIm]Br, Aladdin, Shanghai, China, 97%), H_3PO_4 (85 wt.% aqueous solutions, Aladdin Shanghai, China), the required quantities of aluminum isopropoxide (Aladdin, Shanghai, China, 98%) and iron(III) nitrate nonahydrate (Aladdin, Shanghai, China, 98%) with vigorous stirring. Hydrofluoric acid (HF) (40 wt.% aqueous solution, Sinopharm Chemical Reagent Co., Ltd., Shanghai, China) and cyclohexylamine (Aladdin, Shanghai, China, 98%) were then introduced into the mixture and the final mixture was aging for 1 h before crystallization at 473 K for 90 min under the microwave radiation. Details about the initial reaction mixture composition and the Brunauer–Emmett–Teller (BET) surface area and pore volume of the final products are listed in Table 1. After the crystallization, the samples were washed with deionized water and acetone several times via ultrasonic oscillation and then, dried overnight at 80°C.

2.2. Characterization

The phase purity and the crystallinity of the samples were obtained via powder X-ray diffraction analysis on a Shimadzu XRD-7000S diffractometer (Kyushu, Japan) fitted with Cu-Kα radiation (λ = 1.5418 Å) operating at 40 mA and 40 kV. The morphology of the particles was analyzed via scanning electron microscopy (SEM, Nova NanoSEM 450). Moreover, the textural properties of the calcined samples were determined via nitrogen physisorption at 77 K by using an Autosorb iQ-C adsorption analyzer (Quantachrome Instruments, CT, USA), FL, USA. The surface area was calculated by employing the BET method. UV-Vis diffuse reflectance spectra were obtained from UV-Vis spectrometer (LAMBDA 950, PerkinElmer, CT, USA). Inductively coupled plasma atomic emission spectroscopy (ICP-MS, 7900, Agilent, CA, USA) was employed to measure the concentration of the Fe^{3+}.

2.3. Phenol hydroxylation reaction

In a standard reaction, 2 g of phenol and 0.1 g of catalyst were added to 30 mL of deionized water in a two-neck flask fitted with a condenser. After heating the mixture to 333 k, hydrogen peroxide (H_2O_2, 30 wt.% aqueous solutions) was added through a syringe to the magnetically stirred phenol solution containing (phenol/H_2O_2 = 1/0.8, molar ratio). The reaction results were analyzed on an HPLC Agilent 1100 (Agilent Technologies) equipped with a C8 column (4.6 mm × 150 mm) using a methanol/water mixture (40/60, volume ratio) as the mobile phase at the flow rate of 1.0 mL min^{-1} with UV detection at 277 nm. The identification and quantification of reactants and products were performed using standard compounds include phenol (PH), hydroquinone (HQ) and catechol (CAT).

3. Results and discussion

3.1. Effect of the iron content on the sample structure and performance

Fig. 1 shows the X-ray powder diffraction (XRD) patterns of different samples which greatly matches with the

Table 1
Ionothermal synthesis conditions and their corresponding textural parameters of FeAlPO-34 samples

Samples	xFe_2O_3[a]	BET surface area ($m^2\ g^{-1}$)	Mesopore volume ($cm^3\ g^{-1}$)	Pore volume ($cm^3\ g^{-1}$)
Sample-1	0.05	575	0.210	0.436
Sample-2	0.15	522	0.140	0.379
Sample-3	0.25	497	0.093	0.334
Sample-4	0.35	280	0	0.235

[a]Initial molar composition for the inorganic species is as follows: $Fe_2O_3/Al_2O_3/P_2O_5$/HF cyclohexylamine/[BMIm]Br = $x/(1–x)$/1/2/2/60.

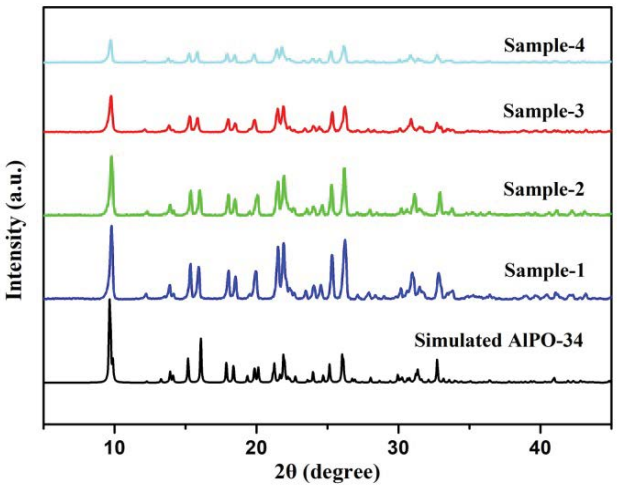

Fig. 1. XRD patterns of synthetic samples with different iron additions and simulated pattern of triclinic CHA-type **AlPO**.

theoretical pattern of triclinic AlPO chabazite (CHA) [20], confirming that the materials are isostructural with AlPO-34. Although the crystallinity of FeAlPO-34 has been reduced from their peak intensity with the increase of the amount of iron, the results indicate that the addition of iron does not change the CHA structure. Meanwhile, a slight left-shifting of peaks could be observed for the FeAlPO-34 samples likely due to the incorporation of iron into the AlPO-34 framework. Besides, no diffraction peaks of mixed oxides were observed from the samples, which indicates that iron species were well dispersed and incorporated into the framework.

To research the environment and distribution of iron ions, the diffuse reflectance UV-Vis spectra of FeAlPO-34 molecular sieves have been deconvoluted into subbands. As shown in Fig. 2, in principle, these samples display strong adsorption bands mainly below 300 nm which assign to isolated Fe^{3+} sites [21]. The band is located above 380 nm which was attributed to a small oligonuler Fe_xO_y cluster in the channel and surface of molecular sieves [22]. Detail atom ratios and the amount of diverse iron species were listed in Table 1. The order of the amounts of isolated octahedral Fe^{3+} species (adsorption bands at around 290 nm) in these samples was as follows: Sample-4 > Sample-3 > Sample-2 > Sample-1, these values suggest that adsorption bands of Fe^{3+} are red-shifted with increasing concentration of iron in the synthesis gel. Although the amount of oligonuclear Fe_xO_y increases with the same order, Sample-4 still has a considerably high content of isolated iron species, compared with other FeAlPOs molecular sieves prepared via hydrothermal or ionothermal method [23].

As shown in Fig. 3, the SEM of the Sample-1 to Sample-4 showed the sphere-like morphology composing of closely packed crystal particles. The average size of nanoparticles increases prominently and the diameter of sphere aggregates increases from 6 to 12 μm when the ratio of the concentration of iron increases from 0.05 wt.% to 0.35 wt.%.

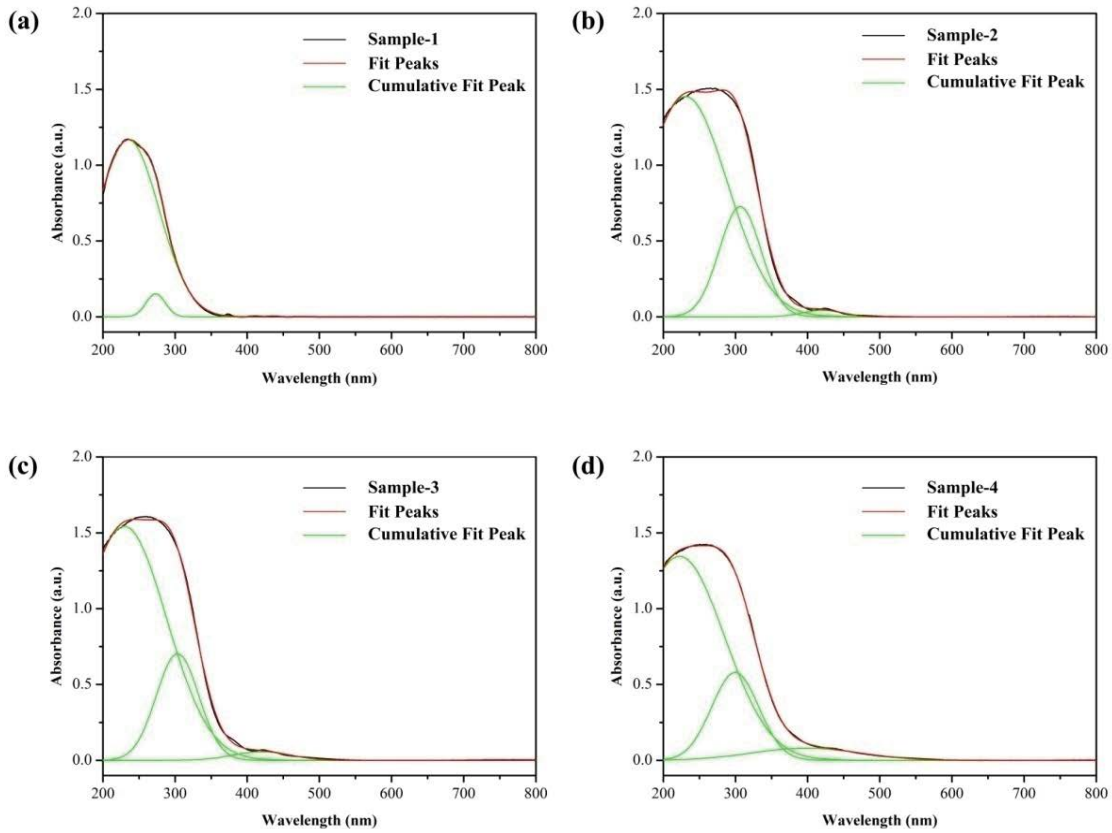

Fig. 2. UV-Vis diffuse reflectance spectra of synthetic samples with different iron additions after deconvolution.

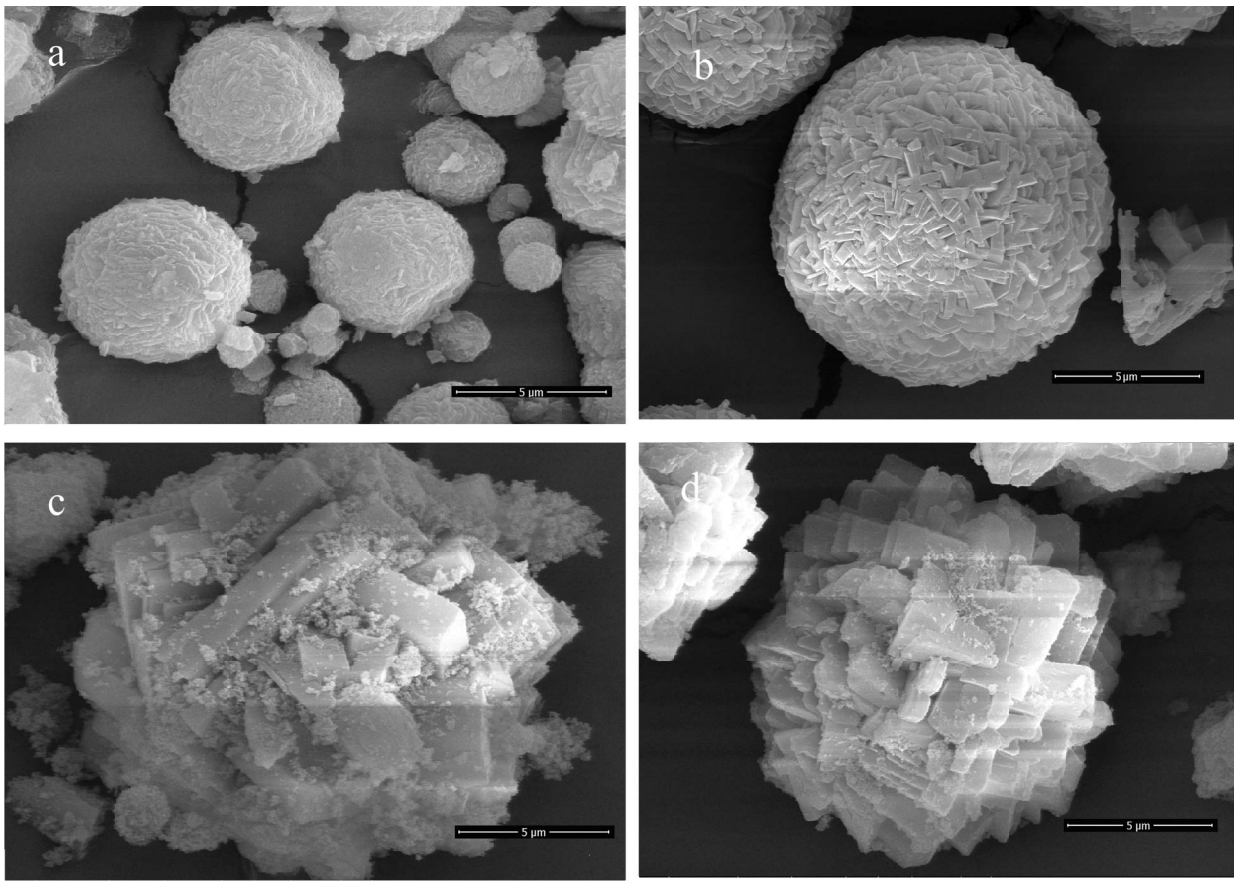

Fig. 3. SEM images of synthetic samples with different iron additions: (a) Sample-1, (b) Sample-2, (c) Sample-3, and (d) Sample-4.

Table 2
Iron content, percentage of Fe species subband areas and phenol hydroxylation catalytic activities of the FeAlPO-34 samples

Sample	Fe (wt.%)	Isolated Fe^{3+a}		Oligonuclear Fe_xO_y A3 (%)[b]	Isolated (wt.%)	Oligonuclear (wt.%)	C_{PH} (mol%)	Selectivity	
		A1 (%)	A2 (%)					(CAT + HQ) (mol%)	CAT/HQ
Sample-1	1.68	95.1	4.9	0	1.68	0	11.16	84.20	7.66
Sample-2	4.00	79.8	18.7	1.5	3.94	0.06	35.81	87.29	2.36
Sample-3	6.09	71.7	25.7	2.6	5.93	0.16	41.55	92.72	1.73
Sample-4	11.62	48.2	40.3	11.5	10.28	1.34	24.78	77.64	2.85

[a]A1 and A2 represent the percentage of subband area at 220 and 290 nm, respectively;
[b]A3 represents the percentage of subband area at 380 nm.

On the basis of ICP-AES and diffuse reflectance UV-Vis analysis, it was concluded that the increase of average size resulted from the amount increase of iron incorporated into the AlPO-34 framework. Besides, a small quantity of amorphous phase can be observed in Fig. 3d, which was consistent with its XRD pattern. Fig. 4 presents the nitrogen adsorption/desorption isothermals of the calcined products with different amounts of iron. Type H4 hysteresis loops can be observed in the range of P/P_0 = 0.4–1.0 in Sample-1, Sample-2 and Sample-3, probably due to the interparticle mesopores of the aggregated particles [24]. It can be observed (Table 1) that their BET surface area and pore volume almost linearly declined with the increase of the amount of Fe ions incorporated into the CHA-structured AlPO-34. In addition, for these three samples, Barrett, Joyner, and Halenda pore size distribution (Figs. 4b–d) appear at about 4 nm, indicating the mesoporous size was almost homogeneous. However, a nearly reversible adsorption–desorption curve which belongs to Sample-4 was observed, demonstrating the sole presence of micropores. Probably due to the incorporation of an excessive amount of iron, the formed oversize crystal particles did not aggregate and then prohibited the generation of mesopores. The findings demonstrate that the initial iron amount not

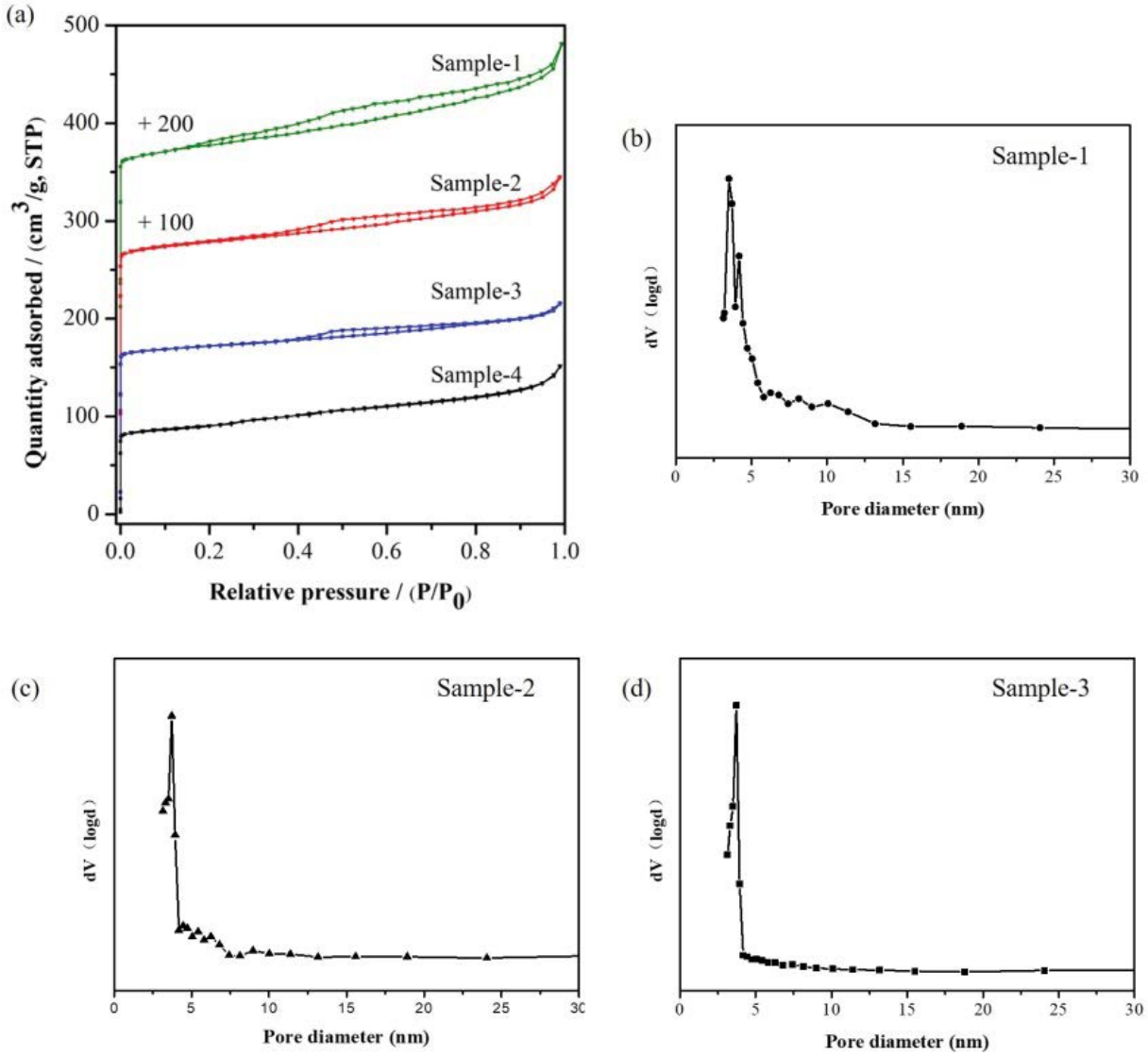

Fig. 4. (a) N_2 physisorption isotherm curves and Barrett, Joyner, and Halenda pore size distribution curves of (a) Sample-1, (b) Sample-2, (c) Sample-3, and (d) Sample-4.

only affects the amount of iron incorporates into the framework, but also affects the molecular sieves morphology and the mesoporous properties.

3.2. Catalytic performance of the FeAlPO molecular sieves

Previous researches have revealed that phenol hydroxylation reaction is supposed to be very sensitive to isolated iron species among plentiful reactions with iron-containing zeolite molecular sieves as a catalyst [25]. The catalytic products, hydroquinone and catechol, are widely used in chemical, pharmaceutical and food industries. The phenol hydroxylation reaction is therefore utilized to measure the catalytic properties of FeAlPO-34 samples with different iron contents and framework iron species. The iron contents of FeAlPO-34 molecular sieves were determined by ICP-AES analysis. As shown in Table 2, the iron content of FeAlPO-34 molecular sieves is proportional to the amount of iron. 1.68 wt.% iron is found in Sample-1, and the iron content keeps increasing with the concentration of iron in the synthesis gel increased. Sample-4 arrived at the highest iron contents, estimated at 11.62 wt.%. Table 2 also displays the catalytic activities of the iron-containing aluminophosphate molecular sieves. Phenol conversions (C_{PH}, mol%) of 11.16, 35.81, 41.55, 24.78 were obtained, with selectivities to HQ and CAT (CAT + HQ) of 84.2, 87.3, 92.72, 77.64 (mol%), respectively. It was the same as previous reports that the activity and selectivity of phenol hydroxylation reaction increased gradually with the increase of the content of isolated tetrahedron coordinated iron species, besides the Sample-4. Sample-4 has the sole presence of micropores and the largest single particle size, thus the majority of active iron species inside the catalyst may not be involved in the reaction. It is generally accepted that the hierarchical structure

Table 3
Catalytic performance of FeAlPO-34 with different cycle times

Cycle times	C_{PH} (%)	Selectivity	
		(CAT + HQ) (mol%)	CAT/HQ
0	41.6	92.7	1.73
1	39.5	86.7	1.81
2	37.1	78.5	1.74
3	34.9	72.7	1.87
4	31.1	61.6	1.65

can significantly enhance the transport rate of bulky molecules and thus bring an excellent catalysis performance [26]. Therefore, excellent catalysis results of these three samples with hierarchical structure and a high amount of isolated coordinated iron species can be well explained.

After the reaction, the mixture was filtered and the residue was calcined at 823 K for 6 h in the air condition for catalyst recycle. After activating treatment, the catalyst was used in the phenol hydroxylation reaction with the same parameter. As shown in Table 3, Sample-3 showed good cycle performance. When the catalyst was recycled 4 times, the phenol conversion was kept at 74.8% and the selectivity of CAT and HQ was 66.5% compared with the initial sample which demonstrated the excellent recycle performance of the FeAlPO-34. The decline of performance may be induced by the blocking of the mesopores and micropores in the zeolite which decreased the effective reaction sites. Also part of the Fe ions may dissolve in the reaction system which affects the active sites also.

4. Conclusions

In conclusion, FeAlPO-34 molecular sieves with high iron contents were successfully fabricated via an ionothermal approach. Based on the results of characterization, mostly iron species are the isolated Fe^{3+} in the FeAlPO-34 framework. Sample-3 with relatively high iron contents and a hierarchical structure shows excellent catalytic performances when utilized as the catalyst of phenol hydroxylation reaction. The sample with 6.09 wt.% Fe showed a 41.55% of phenol conversion with the selectivity of 92.72% to CAT and HQ. When the sample was recycled 4 times, the phenol conversion was kept at 74.8% and the selectivity of CAT and HQ was 66.5% compared with the initial sample. The above results suggest that the ionothermal method in this work provides an efficient approach for the fabrication of high-performance MeAPOs catalyst.

Acknowledgments

The authors wish to thank the Natural Science Fund of China (NO. 21706022), the Science & Technology Program of Jiangxi Provincial Education Bureau (NO. GJJ190557), and Jiangxi Provincial Natural Science Foundation of China (NO. 20202BABL203021) for financial support.

References

[1] M.M. Azim, U. Mohsin, An efficient method for the ionothermal synthesis of aluminophosphate with the LTA framework type, Microporous Mesoporous Mater., 295 (2020) 109957, https://doi.org/10.1016/j.micromeso.2019.109957.
[2] R.L. Han, L. Zhou, Y.W. Luo, Controllable synthesis of Si-DD3R molecular sieves nanocrystalline by microwave assisting dry-gel conversion method, Mater. Res. Express, 7 (2020) 085014.
[3] L. Zhou, R. Han, Y.X. Tao, J.Q. Wang, Y.W. Luo, Optimized preparation of nanosized hollow SSZ-13 molecular sieves with ultrasonic assistance, Nanomaterials, 10 (2020) 2298, https://doi.org/10.3390/nano10112298.
[4] A.C. Martins, R. Fernandez-Felisbino, L.A.M. Ruotolo, Ionothermal synthesis of aluminophosphates used for ion exchange: influence of choline chloride/urea ratio, Microporous Mesoporous Mater., 149 (2012) 55–59.
[5] M.E. Davis, R.F. Lobo, Zeolite and molecular sieve synthesis, Chem. Mater., 4 (1992) 756–768.
[6] Z.L. Liu, M. Xu, X.L. Huai, C.F. Huang, L.T. Lou, Ionothermal synthesis and characterization of $AlPO_4$ and $AlGaPO_4$ molecular sieves with LTA topology, Microporous Mesoporous Mater., 305 (2020) 110315, https://doi.org/10.1016/j.micromeso.2020.110315.
[7] S. Sogukkanli, K. Iyoki, S.P. Elangovan, K. Itabashi, T. Okubo, Seed-directed synthesis of CON-type zeolite using tetraethylammonium hydroxide as a simple organic structure-directing agent, Chem. Lett., 46 (2017) 1419–1421.
[8] C.H. Zhang, Y. Yan, Z.X. Huang, H.Z. Shi, C.Q. Zhang, X.H. Cao, J. Jiang. Triclinic AlPO-34 zeolite synthesized with nicotine and its proton conduction properties, Inorg. Chem. Commun., 96 (2018) 165–169.
[9] P.Y. Feng, X.H. Bu, G.D. Stucky, Hydrothermal syntheses and structural characterization of zeolite analogue compounds based on cobalt phosphate, Nature, 388 (1997) 735–741.
[10] W. Fortas, A. Djelad, M.A. Hasnaoui, M. Sassi, A. Bengueddach, Adsorption of gentian violet dyes in aqueous solution on microporous AlPOs molecular sieves synthesized by ionothermal method, Mater. Res. Express, 5 (2018) 025018.
[11] E.R. Cooper, C.D. Andrews, P.S. Wheatley, P.B. Webb, P. Wormald, R.E. Morris, Ionic liquids and eutectic mixtures as solvent and template in synthesis of zeolite analogues, Nature, 430 (2004) 1012–1016.
[12] E.J. Fayad, N. Bats, C.E.A. Kirschhock, B. Rebours, A.-A. Quoineaud, J.A. Martens, A rational approach to the ionothermal synthesis of an $AlPO_4$ molecular sieve with an lta-type framework, Angew. Chem. Int. Ed., 49 (2010) 4585–4588.
[13] H. Liu, Z.J. Tian, L. Wang, Y.S. Wang, D.W. Li, H.J. Ma, R.S. Xu, Ionothermal synthesis of MnAPO-SOD molecular sieve without the aid of organic structure-directing agents, Inorg. Chem., 55 (2016) 1809–1815.
[14] L.J. Han, Y.B. Wang, C.X. Li, S.J. Zhang, X.M. Lu, M.J. Cao, Simple and safe synthesis of microporous aluminophosphate molecular sieves by ionothermal approach, AIChE J., 54 (2008) 280–288.
[15] N.R. Shiju, S. Fiddy, O. Sonntag, M. Stockenhuber, G. Sankar, Selective oxidation of benzene to phenol over FeAlPO catalysts using nitrous oxide as oxidant, Chem. Commun., 47 (2006) 4955–4957.
[16] L.P. Zhou, J. Xu, H. Miao, X.Q. Li, F. Wang, Synthesis of FeCoMnAPO-5 molecular sieve and catalytic activity in cyclohexane oxidation by oxygen, Catal. Lett., 99 (2005) 231–234.
[17] C.X. Fang, X.M. Gao, X.C. Zhang, J.H. Zhu, S.-P. Sun, X.N. Wang, W.D. Wu, Z.X. Wu, Facile synthesis of alkaline-earth metal manganites for the efficient degradation of phenolic compounds via catalytic ozonation and evaluation of the reaction mechanism, J. Colloid Interface Sci., 551 (2019) 164–176.
[18] R.L. Han, M. Chen, X.B. Liu, Y.H. Zhang, Y.L. Xie, Y. Sui, Controllable synthesis of Mn_3O_4 nanowires and application in the treatment of phenol at room temperature, Nanomaterials, 10 (2020) 461, https://doi.org/10.3390/nano10030461.
[19] R.L. Han, Y.H. Zhang, Y.L. Xie, Application of Mn_3O_4 nanowires in the dye waste water treatment at room temperature, Sep.

Purif. Technol., 234 (2020) 116119, https://doi.org/10.1016/j.seppur.2019.116119.
[20] M.M. Harding, B.M. Kariuki, Microcrystal structure determination of $AlPO_4$-CHA using synchrotron radiation, Acta Crystallogr., Sect. C: Cryst. Struct. Commun., 50 (1994) 852–854.
[21] L.D. Li, Q. Shen, J.J. Yu, Z.P. Hao, Z.P. Xu, G.Q. Max Lu, Fe–USY zeolite catalyst for effective decomposition of nitrous oxide, Environ. Sci. Technol., 41 (2007) 7901–7906.
[22] J. Perez-Ramirez, J.C. Groen, A. Brückner, M.S. Kumar, U. Bentrup, M.N. Debbagh, L.A. Villaescusa, Evolution of isomorphously substituted iron zeolites during activation: comparison of Fe-beta and Fe-ZSM-5, J. Catal., 232 (2005) 318–334.
[23] X.H. Zhao, H. Wang, B.F. Dong, Z.P. Sun, G.X. Li, X.L. Wang, Facile synthesis of FeAlPO-5 molecular sieve in eutectic mixture via a microwave-assisted process, Microporous Mesoporous Mater., 151 (2012) 56–63.
[24] O. Sel, D.B. Kuang, M. Thommes, B. Smarsly, Principles of hierarchical meso- and macropore architectures by liquid crystalline and polymer colloid templating, Langmuir, 22 (2006) 2311–2322.
[25] X.H. Zhao, X.X. Zhang, Z.X. Hao, X.P. Gao, Z. Liu, Synthesis of FeAPO-5 molecular sieves with high iron contents via improved ionothermal method and their catalytic performances in phenol hydroxylation, J. Porous Mater., 25 (2017) 1007–1016.
[26] J. Pérez-Ramírez, C.H. Christensen, K. Egeblad, C.H. Christensen, J.C. Groen, Hierarchical zeolites: enhanced utilisation of microporous crystals in catalysis by advances in materials design, Chem. Soc. Rev., 37 (2008) 2530–2542.